SUPPLEMENTAL METHODS

Cell culture

MM cell lines were maintained in RPMI 1640 medium supplemented with 10% fetal calf serum (Hyclone) and penicillin/ streptomycin (Invitrogen) with or without 10 ng/mL interleukin-6 (R&D Systems)[1].

FISH analyses

Metaphase and interphase FISH with locus-specific and chromosome painting probes were performed on MMCL VP6, MM-M1, XG2, KP6, MOLP8, JIM3, JJN3, and EJM. The following probes were described elsewhere: CH BAC, MYC BAC (GS-93F05), MYC plasmid[1]. Other BAC and fosmid clones were identified through the Human Genome Browser (hg19 assembly) based on the genomic positions of the DNA fragments (Table S3), and were obtained from the BACPAC Resources (Oakland, CA) and Life Technologies (Thermo Fisher Scientific). Probes were labeled by nick translation with either biotin-16-dUTP (Roche, Indianapolis, IN) followed by avidin-FITC (Sigma, St. Louis, MO) detection or digoxigenin-11-dUTP (Roche, Indianapolis, IN) followed by TRITC antibody (Sigma, St. Louis, MO) detection. Whole chromosome painting probes were generated by direct PCR labeling with Cy5-dUTP of chromosome-specific template DNA. Slide pretreatment, hybridization and detection procedure were described elsewhere [1]. Image acquisition was accomplished using Leica DMXRA fluorescence microscope with CCD camera (Sensys, Photometrics) and LEICA QFISH software.

Comparative genomic hybridization

The Agilent 244K CGH data were downloaded from the Multiple Myeloma Genomics Portal (http://www.broad.mit.edu/mmgp). The Agilent 244K CGH data were segmented using circular binary segmentation implemented in the R/Bioconductor package DNA copy (Seshan & Olshen 2015). All genomic coordinates are from hg19**.**

Enhancer prediction

We identified potential enhancer elements by the presence of conventional enhancer and super-enhancer chromatin marks in the MM.1S MMCL as predicted by others [2, 3]. For the GM12878 lymphoblastoid cell line (LCL), which is phenotypically similar to MM cell lines, putative conventional enhancers were identified from ENCODE data on the UCSC genome browser (http://genome.ucsc.edu)[4], whereas others had identified super-enhancers [2] and stretch enhancers [5].

Copy number variation from whole genome sequencing data.

The CNV from the whole genome sequencing data for 35 BRCA tumors (Table S4) was calculated using a Mayo in-house developed algorithm. Briefly, the regional sequencing depths of a 10-kb sliding window were calculated from BAM files using only specifically mapped reads (MAPQ $\geq$ 30). The genomic regions of repeats and/or low mappabilities were masked based on the UCSC GoldenPath database, and the GC bias from region to region was corrected using a smooth-spline model. The sequencing depths of

each sample were normalized and the CNV regions were called using the circular binary segmentation methods [6].

SRA link for mate pair sequences for MMCLs and 25 primary myeloma tumors

ftp://ftp-trace.ncbi.nlm.nih.gov/sra/review/SRP064107_20160427_134403_149dd5056939405870c9bb50cbc8691c

SUPPLEMENTAL REFERENCES

1. Gabrea, A., et al., Secondary genomic rearrangements involving immunoglobulin or MYC loci show similar prevalences in hyperdiploid and nonhyperdiploid myeloma tumors. Genes Chromosomes Cancer, 2008. **47**(7): p. 573-90.
2. Hnisz, D., et al., Super-enhancers in the control of cell identity and disease. Cell, 2013. **155**(4): p. 934-47.
3. Loven, J., et al., Selective inhibition of tumor oncogenes by disruption of super-enhancers. Cell, 2013. **153**(2): p. 320-34.
4. Ernst, J., et al., Mapping and analysis of chromatin state dynamics in nine human cell types. Nature, 2011. **473**(7345): p. 43-9.
5. Parker, S.C., et al., Chromatin stretch enhancer states drive cell-specific gene regulation and harbor human disease risk variants. Proc Natl Acad Sci U S A, 2013. **110**(44): p. 17921-6.
6. Olshen, A.B., et al., Circular binary segmentation for the analysis of array-based DNA copy number data. Biostatistics, 2004. **5**(4): p. 557-72.

SUPPLEMENTAL FIGURE LEGENDS AND LIST OF TABLES

Figure S1. Four other examples of complex MYC locus rearrangements in MMCL.
A) MM-M1; B) Karpas 620; C) KMS34. See Fig. 1,2,3 and text for additional details.

Figure S2. Copy number abnormalities in the *MYC* locus in MM tumors and cell lines Segmented Agilent 244K aCGH of the *MYC* locus (chr8:126,000,000–130,000,000) in 2 MM tumors and 11 MMCLs with copy numbers abnormalities viewed in IGV is shown. The overall copy number for the region for each sample has been normalized to two copies to highlight local changes in copy number. More than 1 log2 gain is in deep red, more than 1 log loss is in deep blue and copy number within 0.2 log of diploid is in white.

Figures S3. Four other examples of complex non-MYC locus rearrangements in MMCL. A) XG2. Chr20 (CD40 gene) inserted into Chr22 duplicated sequences (IGL); B) XG2, Chr 22 (IGL) inserted into Chr20 duplicated sequences (MAFB); C) XG2, t(12;14) translocation; D) JIM3, chr20 inversion. See text

for additional details.

Figure S4. Sizes of duplications breakpoint junctions in MMCL.
TD, 161 tandem duplications; IC.DUP, 20 duplications with interchromosmal insertions or translocations; INV.DUP, 9 duplications with inversions. See text for additional details.

Table S1. *MYC* locus breakpoints in 12 MMCL.

Table S2. Reciprocal interchromosomal and inversion breakpoints in eight MMCL.

Table S3. Reciprocal interchromosomal breakpoints in 25 primary myeloma tumors

Table S4. Reciprocal interchromosomal breakpoints in 140 tumors

Table S5. Locations of FISH probes not previously published.

Figure S1.

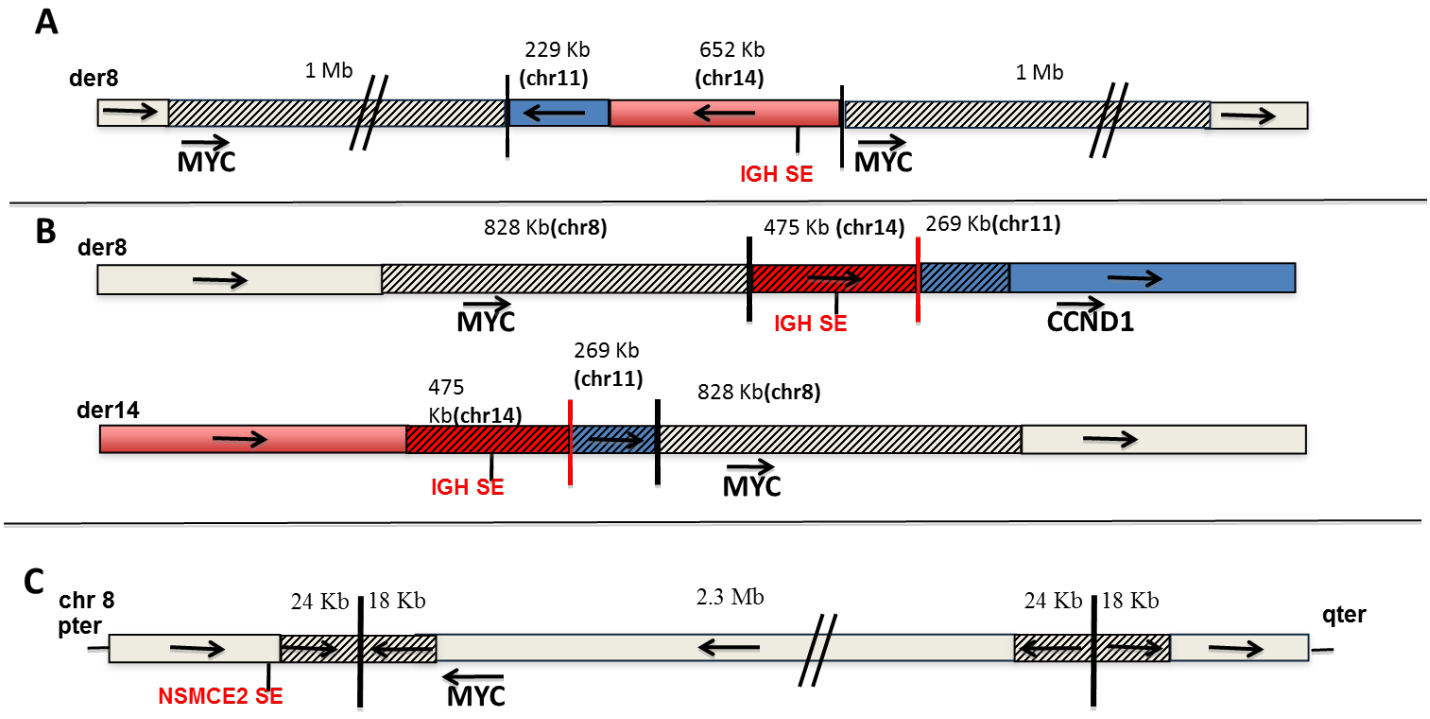

Figure S2.

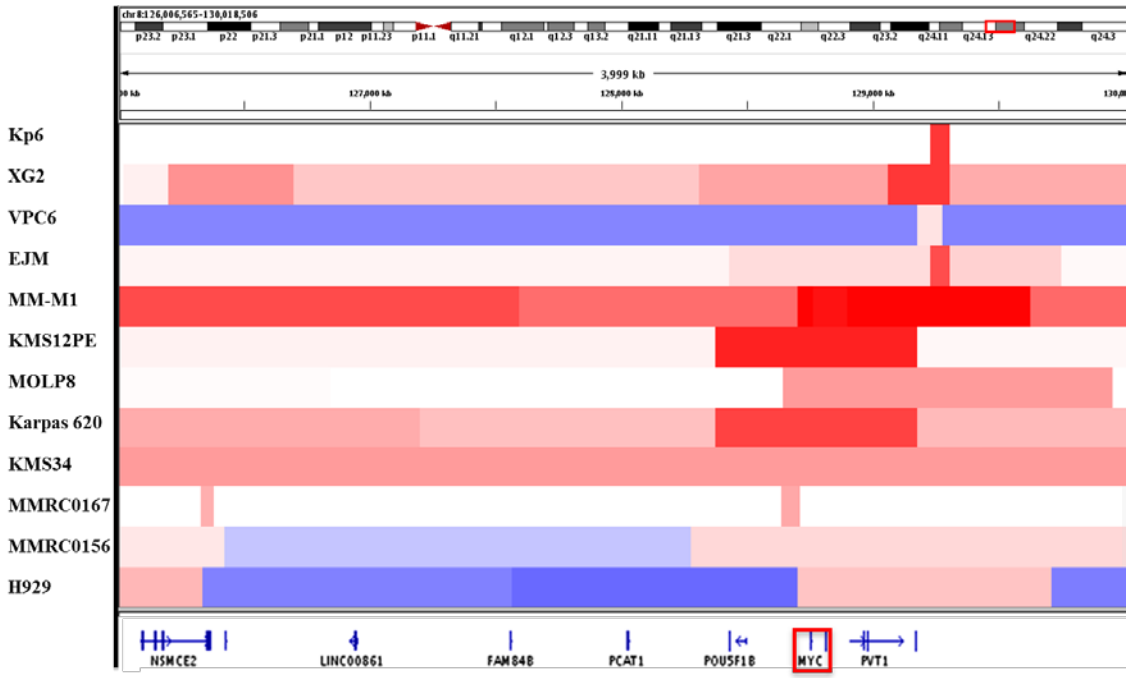
chr8:126,006,565-130,018,506
3,999 kb
Kp6
XG2
VPC6
EJM
MM-M1
KMS12PE
MOLP8
Karpas 620
KMS34
MMRC0167
MMRC0156
H929
NSMCE2
LINC00861
FAM84B
PCAT1
POU5F1B
MYC
PVT1

Figure S3.

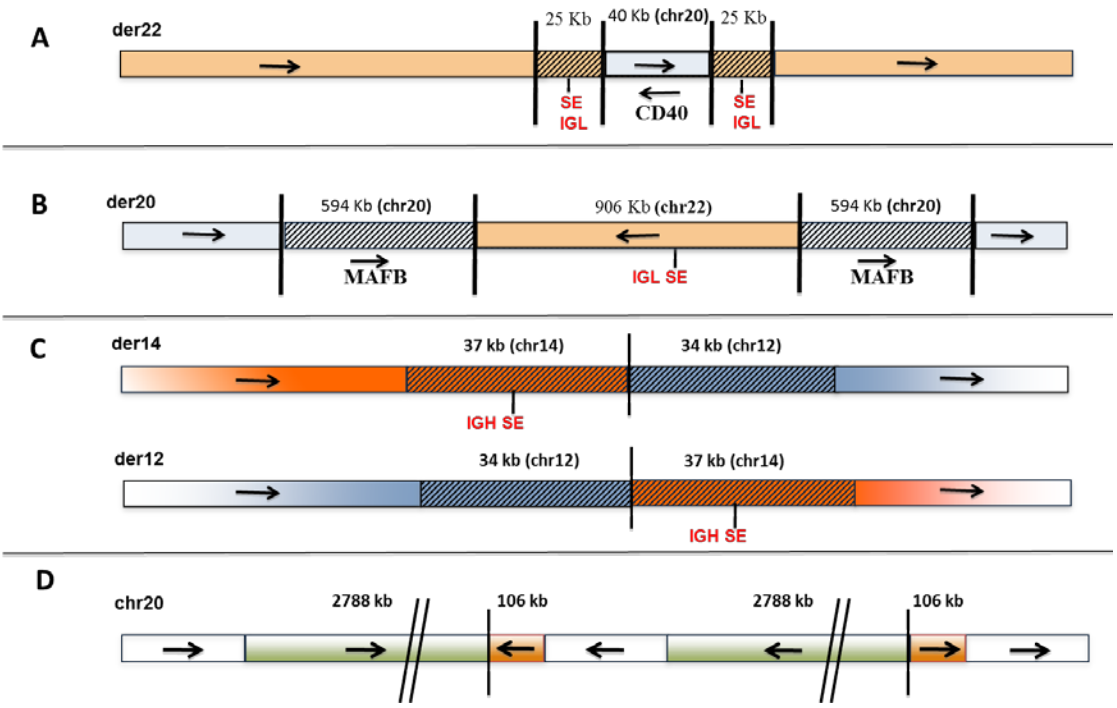

Figure S4.

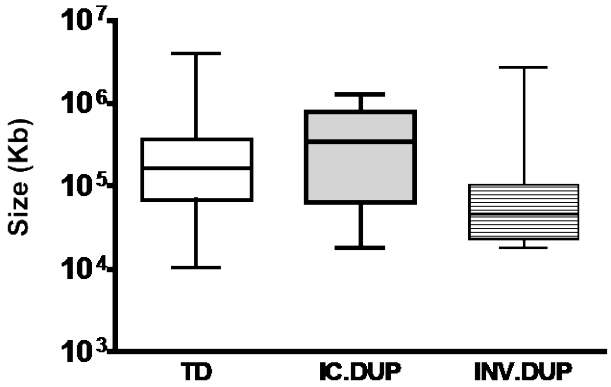

Table S1. *MYC* locus breakpoints in 12 MMCL

MMCL	Rearrangement (type)	Partner chromosomes	Breakpoint locations (hg19)	Determined by
KP6	Tandem duplication	8	8:129,239,488- / 8:129,329,926+	breakpoint sequence
XG2	Tandem duplication	8	8:129,072,697- / 8:+129,413,553	breakpoint sequence
EJM	Insertion	8(11)	8:129,346,425+ / 11: 62,245,125+	breakpoint sequence
			8:129,265,218- / 11: 62,187,330-	breakpoint sequence
VP6	Insertion	8(14)	8:129,305,155+ / 14:106,084,351-	breakpoint sequence
			8:129,216,248- / 14:106,114,212 +	breakpoint sequence
Karpas 620	Translocation	8/11/14	14: 106,327,463+ / 11:69,065,284-	breakpoint sequence
			~ 8:128,379,000- / ~11: 69,374,000+	CGH
			~8: 129,182,000+ /~ 14:105,772,000-	CGH
MOLP8	Insertion	4(8/11/14)	8: 128,690,954- / 4:38,172,506-	mate pair (2.5 kb)
			8: 129,989,725+ / 11:69,452,569+	mate pair (2.5 kb)
			14: 105,751,601- / 4:39,480,472+	mate pair (2.5 kb)
			11:69,065,588-/ 14:106,174,817+	mate pair (2.5 kb)
MM-M1	Insertion	8(/11/14)	8: 128,708,505- / 14:105,673,285-	mate pair (2.5 kb)
			8: 129,675,098+ / 11: 69,295,289+	mate pair (2.5 kb)
			14: 106,328,066+ / 11:69,070,470-	mate pair (2.5 kb)
KMS12	Insertion	8(11/14)	8: 128,388,987- / 11:69,295,045+	mate pair (5 kb)
			8: 129,217,712+ / 14: 105,665,924-	mate pair (5 kb)
			11: 69,139,832- / 14: 106,112,663+	mate pair (5 kb)
KMS34	Inversion	8	8: 126, 338, 467- / 8:128,752,633-	mate pair (2.5 kb)
			8; 126,362,626+ /8:128,770,829+	mate pair (2.5 kb)
H929	Deletion	8	8:126,344,413+ / 8:128,713,155-	mate pair (2.5 kb)
8226	Insertion	16/22(2/8)	16: 79,966,477+ / 22:23,264,974-	mate pair (2.5 kb)
			8: 128,739,150- / 22:23,289,814+	mate pair (2.5 kb)
			8: 128,818,377+ / 2:134,827,514-	mate pair (2.5 kb)
			2:134,910,943+/ 16:79,869,474-	mate pair (2.5 kb)
JIM3	Translocation	6/8	6:103,707,216-/ 8:128,798,915+	mate pair (2.5 kb)
			6:104,468,603+/ 8:128,733,865-	mate pair (2.5 kb)